White Rose Research Online

eprints@whiterose.ac.uk
https://eprints.whiterose.ac.uk
Universities of Leeds, Sheffield and York

Deposited via The University of York.

White Rose Research Online URL for this paper:
https://eprints.whiterose.ac.uk/id/eprint/122585/

Version: Accepted Version

Article:
Hallam, Glyn Paul, Thompson, Hannah Elizabeth, Hymers, Mark et al. (2017) Task-based and resting-state fMRI reveal compensatory network changes following damage to left inferior frontal gyrus. Cortex. ISSN: 1973-8102

https://doi.org/10.1016/j.cortex.2017.10.004

Reuse
This article is distributed under the terms of the Creative Commons Attribution-NonCommercial-NoDerivs (CC BY-NC-ND) licence. This licence only allows you to download this work and share it with others as long as you credit the authors, but you can't change the article in any way or use it commercially. More information and the full terms of the licence here: https://creativecommons.org/licenses/

Takedown
If you consider content in White Rose Research Online to be in breach of UK law, please notify us by emailing eprints@whiterose.ac.uk including the URL of the record and the reason for the withdrawal request.

Title: Task-based and resting-state fMRI reveal compensatory network changes following damage to left inferior frontal gyrus

Running title: Compensatory semantic control following left prefrontal damage

Authors: Glyn P. Hallam[1,5]*, Hannah E. Thompson[6], Mark Hymers[1], Rebecca E. Millman[2], Jennifer M. Rodd[3], Matthew A. Lambon Ralph[4], Jonathan Smallwood[1] Elizabeth Jefferies[1]

[1]Department of Psychology and York Neuroimaging Centre, University of York, York, YO10 5DD, UK

[2]Manchester Centre for Audiology and Deafness, School of Health Sciences, Faculty of Biology, Medicine and Health, University of Manchester, Manchester, M13 9PL, UK

[3]Department of Experimental Psychology, University College London, 26 Bedford Way, London, WC1H 0AP, UK

[4] Neuroscience and Aphasia Research Unit (NARU), Division of Neuroscience and Experimental Psychology, School of Biological Sciences, University of Manchester, UK

[5] Department of Psychology, School of Human and Health Sciences, University of Huddersfield, Huddersfield, HD1 3DH

[6] School of Psychology, University of Surrey, Guildford, GU2 7XH

*Correspondence to: Department of Psychology, School of Human and Health Sciences, University of Huddersfield, Huddersfield, HD1 3DH, United Kingdom, e-mail: g.hallam@hud.ac.uk

Abstract

Damage to left inferior prefrontal cortex in stroke aphasia is associated with semantic deficits reflecting poor control over conceptual retrieval, as opposed to loss of knowledge. However, little is known about how functional recruitment within the semantic network changes in patients with executive-semantic deficits. The current study acquired fMRI data from 14 patients with semantic aphasia, who had difficulty with flexible semantic retrieval following left prefrontal damage, and 16 healthy age-matched controls, allowing us to examine activation and connectivity in the semantic network. We examined neural activity while participants listened to spoken sentences that varied in their levels of lexical ambiguity and during rest. We found group differences in two regions thought to be good candidates for functional compensation: ventral anterior temporal lobe (vATL), which is strongly implicated in comprehension, and posterior middle temporal gyrus (pMTG), which is hypothesized to work together with left inferior prefrontal cortex to support controlled aspects of semantic retrieval. The patients recruited both of these sites more than controls in response to meaningful sentences. Subsequent analysis identified that, in control participants, the recruitment of pMTG to ambiguous sentences was inversely related to functional coupling between pMTG and anterior superior temporal gyrus (aSTG) at rest, while the patients showed the opposite pattern. Moreover, stronger connectivity between pMTG and aSTG in patients was associated with better performance on a test of verbal semantic association, suggesting that this temporal lobe connection supports comprehension in the face of damage to left inferior prefrontal cortex. These results characterize network changes in patients with executive-semantic deficits and converge with studies of healthy participants in providing evidence for a distributed system underpinning semantic control that includes pMTG in addition to left inferior prefrontal cortex.

Keywords

Semantic control; fMRI; resting-state connectivity; sentence processing; functional compensation

1.0 Introduction

Semantic cognition – the application of conceptual knowledge to drive appropriate thought and behaviour – is critical for many aspects of functioning, including the capacity to understand and use objects, and the production and comprehension of language (Lambon Ralph et al., 2017). The study of patients with different varieties of semantic impairment has suggested that distinct brain regions support different aspects of semantic cognition (Jefferies, 2013; Jefferies & Lambon Ralph, 2006). Patients with semantic dementia (SD) exhibit a gradual degradation of conceptual knowledge across modalities following atrophy focused on the ventral anterior temporal lobes (vATL) (Bozeat et al., 2000; Patterson et al., 2007). Patients with semantic aphasia (SA) can also show multimodal semantic deficits following infarcts in left frontal or temporoparietal areas: they appear to have difficulty accessing knowledge in a flexible and task-appropriate way, while the store of semantic information, supported by the vATL, is largely spared (Jefferies & Lambon Ralph, 2006; Rogers et al., 2016). SA patients are strongly influenced by the control requirements of semantic tasks and are much more sensitive than SD patients to cues that reduce the need for internally-generated constraints on semantic retrieval (Jefferies et al., 2007; Corbett et al., 2011). Patients with SA produce errors when strong distracters are present, generate task-irrelevant yet highly-associated responses in picture naming, and find it difficult to retrieve non-dominant knowledge, including the subordinate meanings of ambiguous words (Noonan et al., 2010; Corbett et al., 2011).

Patients with SA typically have large left-hemisphere lesions showing maximal overlap in left inferior frontal gyrus (LIFG), and often extending into temporoparietal regions, including posterior middle temporal gyrus (pMTG; Thompson et al., 2015). Furthermore, there are reports of patients with damage restricted to temporoparietal cortex who show similar deficits to those with LIFG lesions (Jefferies & Lambon Ralph, 2006; Berthier, 2001). Functional neuroimaging and transcranial magnetic stimulation studies of healthy participants suggest that both left inferior frontal gyrus (LIFG) and posterior middle temporal gyrus (pMTG) support the flexible controlled retrieval of semantic information. Both of these regions show stronger activation across a range of manipulations of semantic control, including distractor strength,

ambiguity, and the strength of the relationship being probed (Badre et al., 2005; Davey et al., 2015a; 2016; Noonan et al., 2013; Whitney et al., 2011a). Similarly, the application of inhibitory TMS to either left LIFG or pMTG disrupts difficult semantic judgements in which target meanings are relatively weak or ambiguous (Whitney et al., 2011b; Hoffman et al., 2010; Davey et al. 2015b). These findings help to explain why damage to left posterior temporal and inferior prefrontal cortex can elicit similar semantic deficits in patients with SA (Noonan et al., 2010; Corbett et al., 2011). Tractography and resting-state fMRI studies have also shown that there are strong, direct white matter connections and functional connectivity between the IFG and pMTG (JeYoung & Lambon Ralph, 2016).

These findings from neuropsychology, neuroimaging and neurostimulation are consistent with a component process account of semantic cognition in which transmodal conceptual representations supported by the ventral ATL interact with control processes that recruit LIFG and pMTG (Jefferies, 2013; Jefferies & Lambon Ralph, 2006; Noonan et al., 2013; Lambon Ralph et al., 2017). While this framework provides a useful account of the dissociation between SD and SA, the way in which these neurocognitive components are recruited flexibly to support comprehension is poorly understood. There have been few, if any, fMRI studies of the neural basis of residual comprehension in patients with SA and thus it is not known whether these patients show a different pattern of recruitment and/or changes in connectivity within the functional network specifically implicated in semantic control (e.g., stronger activation of left pMTG in patients with damage to left prefrontal cortex), in other parts of the semantic system implicated in conceptual representation, such as ventral ATL, or within aspects of the semantic network particularly allied to the task being performed, for example, superior temporal gyrus for sentence-listening tasks (e.g. Scott et al., 2000). Robson et al. (2013) found that increased vATL activation was linked to levels of comprehension in patients with Wernicke's aphasia. Patients showed significantly greater bilateral ATL activation compared to controls; controls also showed enhanced activation of ATL in a more demanding semantic decision task, suggesting that upregulation of ATL regions is an inherent mechanism in the healthy brain. However, in patients with semantic control deficits, other forms of compensation may be as or more important. For example,

a recent study found that inhibitory TMS to LIFG in healthy participants increased the response within pMTG during a semantic task, particularly for high-control judgements (Hallam et al., 2016), suggesting that damage to LIFG in SA may elicit a stronger response in pMTG during semantic processing.

Here, we examined neural recruitment related to semantic processing in SA patients and age-matched controls, using task-based fMRI and resting-state functional connectivity, to characterize how the response within the semantic network differs in patients with executive-semantic deficits. We compared the brain's response to auditory sentences and spectrally-rotated speech (SRS; Blesser, 1972), to identify the network underpinning naturalistic comprehension in the absence of explicit task instructions. This contrast activates a processing stream along the superior temporal gyrus and into ATL (Scott, Blank, Rosen & Wise, 2000), as well as regions of ventral prefrontal and inferior-to-middle temporal cortex that respond to meaning ambiguity and other manipulations of semantic control (Noonan et al., 2013; Rodd et al., 2005, 2012; Vitello et al., 2014). We used auditory presentation to avoid additional demands related to reading, plus a "sparse" fMRI data acquisition sequence that limits contamination of neural signals by scanner noise.

Using these data, we examined how SA patients with lesions in left prefrontal cortex respond to sentences relative to controls in undamaged parts of the semantic network. We focused on two key regions. First, we examined the response within vATL, which is considered to be a key region for the representation of heteromodal aspects of conceptual knowledge. If upregulation of this region is a general response to increased difficulty of semantic tasks, we would expect increased activation within this region in patients with SA (see above). Secondly, we characterized the response within pMTG, which co-activates with LIFG to support semantic control in healthy participants. We hypothesized that this region might also show a stronger response to the presentation of ambiguous sentences if undamaged parts of the semantic control network become more critical for comprehension following damage to left prefrontal cortex. We also acquired task-free resting state scans that allowed us to characterize connectivity differences for brain regions relevant to semantic processing in patients and controls. We predicted that differences in recruitment might be

reflected in the functional organization of key nodes of the semantic system measured at rest: for example, pMTG might show stronger connectivity to other regions relevant for semantic processing in participants who also show greater activation of this region following an infarct in the left prefrontal cortex. Finally, we examined whether these differences in connectivity related in a positive or negative fashion to semantic performance outside the scanner. Although differences in neural organization following brain injury might support comprehension, these effects might also be the consequence of semantic difficulties (and therefore show the opposite correlation with behaviour).

2.0 Materials and Methods

2.1 Participants

The study was approved by the local Research Ethics Committee. Fourteen patients broadly meeting the definition of semantic aphasia used by Jefferies & Lambon Ralph (2006) – i.e., with multimodal comprehension impairment – were recruited from local stroke and communication support groups (9 females, mean age = 61, SD = 11), together with 16 age- and education-matched neurologically healthy controls (9 females, mean age = 64, SD = 9). Although some of the patient participants in this study presented with milder deficits than those reported by Jefferies & Lambon Ralph (2006) – i.e., they were not impaired on the Camel and Cactus test tapping word and picture semantic associations (further details in Table 1 below) – every case was below the normal cut-off on a more demanding verbal semantic task (comprehending the non-dominant meanings of ambiguous words). The patients were also impaired on a demanding non-verbal semantic task (involving understanding the non-canonical uses of objects, presented as photographs, although data is missing for two patients – one of whom did show a deficit on picture Camel and Cactus judgements; further details below and in Figure 1). All patients and control participants gave written informed consent as approved by the Research Ethics Committee NHS ethics committee. All the patients had chronic deficits arising from a cerebrovascular accident affecting left frontal cortex (typically along with other brain regions) at least one year before the study. Table 1 shows demographic details, neuropsychological profile and

aphasia classification of the participants. The typical lesion in this sample is shown in Figure 2 and further details about the brain regions damaged in individual patients is shown in the Supplementary Materials (Figure S1).

2.2 Neuropsychological assessment

Background neuropsychological testing included assessments of semantic cognition (both verbal and non-verbal tasks), language and executive function.

(i) To characterize semantic processing in a way that would allow the participants in this study to be compared with other individuals with aphasia, we report data from standard semantic tests. We used basic-level picture naming, word-picture matching, verbal and non-verbal association judgements (Camel and Cactus Test) and category fluency (8 categories) from the Cambridge semantic battery (Bozeat et al., 2000), which assesses verbal and non-verbal comprehension and speech production for the set of 64 same concepts. Word-picture matching involved an array of ten semantically-related items, while the association judgements required a probe to be matched with one of four response options, presented as either pictures or words (in written form and also spoken aloud by the researcher). Twelve of the patients were impaired on at least one of these tasks (see Table 1).

(ii) To assess aspects of semantic aphasia already reported in the literature, we employed three additional semantic tasks. (i) We compared the comprehension of dominant (e.g., bark-dog) and non-dominant (e.g., bark-tree) interpretations of ambiguous words in a four-alternative forced-choice task (see Noonan et al., 2010 for further details of the task). All but one of the patients (Case 8) were highly sensitive to this manipulation (see Figure 1). (ii) In an object use task, we examined the ability to identify an object that could be used to achieve a goal (depicted in words and pictures – e.g., "kill a fly", with a photograph of a fly on the table). In the "canonical use" condition, the target was an object whose sole or typical use was to achieve the goal (e.g., fly swat). In the "alternative use" condition,

the target object had the right properties to achieve the goal but this was not its typical function (e.g., a rolled-up newspaper – normally associated with reading). There were six response options (see Corbett et al., 2011 for further details of the task). All of the patients were sensitive to this manipulation (see Figure 1). These combined results confirmed that our sample of SA patients was especially impaired at retrieving non-dominant aspects of meaning across verbal and non-verbal tasks, and thus they resembled patients studied previously. (iii) In synonym judgement, a probe word was presented with three response options. The words on each trial varied in lexical frequency and imageability (full task details in Jefferies et al., 2009). Patients with semantic aphasia, in common with those with "access" impairment, typically show insensitivity to frequency/familiarity (Jefferies et al., 2007; Warrington & Cipolotti, 1996; Thompson et al., 2015; Hoffman, Rogers and Lambon Ralph, 2011). This pattern was observed in our patient sample, in all but one of the individual patients (Patient 3; see Figure 1).

(iii) To characterize other aspects of language processing, we examined words per minute on the Cookie Theft picture description task (BDAE; Goodglass & Kaplan, 1983) and word repetition (Test 7) from the PALPA (Psycholinguistic Assessments of Language Processing in Aphasia; Kay, Lesser & Coltheart, 1992). Since our only inclusion criteria was multimodal semantic deficit in the context of stroke aphasia, the patients had a range of other language impairments (e.g., deficits in repetition and fluency of speech), but their comprehension problems could not be entirely accounted for in these terms (since they extended to picture-based tasks, see above). Moreover, since the patients had largely intact performance on word-picture matching (with only patient 4 scoring substantially below normal limits), we considered that basic auditory processes required to access meaning from spoken words (i.e., in our fMRI sentence listening paradigm) were largely preserved.

(iv) To document the possible contribution of non-semantic deficits in cognitive control to semantic processing, we assessed executive function and non-verbal reasoning with Raven's progressive coloured matrices test (Raven, 1962) and Brixton rule attainment test (Burgess & Shallice, 1997). Raven's matrices requires participants to identify which of six tiles can be used to complete a pattern, and provides a nonverbal estimate of fluid intelligence. The Brixton Rule Attainment test is a visuospatial task which involves anticipating where a coloured dot will move within a grid, requiring the ability to detect rules in sequences of stimuli. Nine of the group showed deficits on at least one of these assessments. These findings are in line with Jefferies and Lambon Ralph (2006), who showed that semantic deficits in semantic aphasia were correlated with executive dysfunction (unlike the impairment in semantic dementia).

Figure 1: Deficits of semantic control and access in the current sample of SA patients

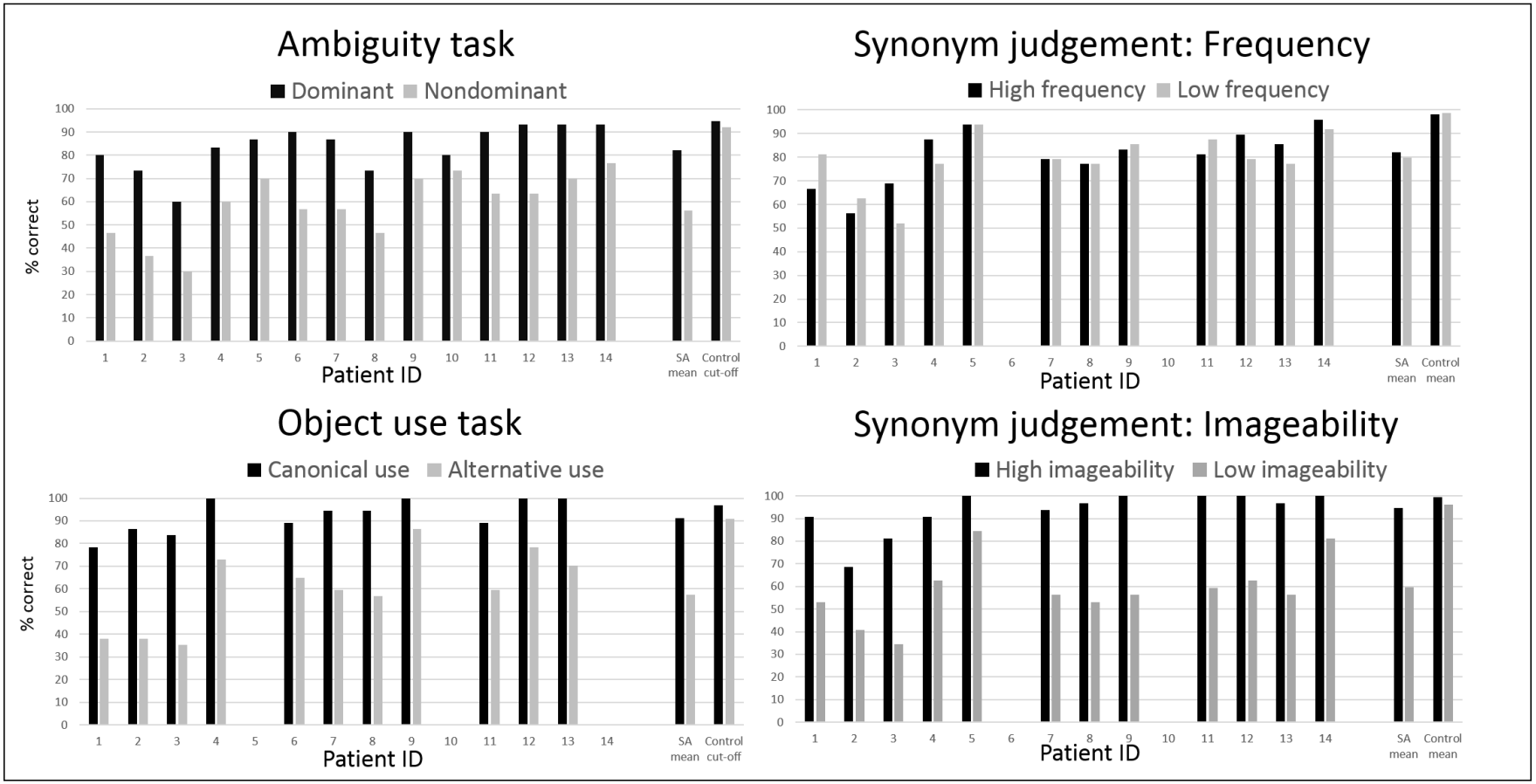

Impairment on a variety of semantic control tasks in the patient sample. Patients are ordered by severity of semantic impairment (score on the Camel and Cactus test). Ambiguity task is taken from Noonan et al., 2010; Object use task is taken from Corbett et al., 2009; synonym judgement task is taken from Jefferies et al., 2010. A semantic control deficit was defined on the basis of below cut-off performance on the non-dominant interpretations of ambiguous words (demonstrating verbal comprehension impairment), plus below cut-off performance in understanding the non-canonical uses of objects (demonstrating non-verbal comprehension impairment). All patients in the group met these inclusion criteria (although data is missing for two patients in the object use task).

Table 1 – Demographic details and background neuropsychology

	Max	Cut-off	1	2	3	4	5	6	7	8	9	10	11	12	13	14
Age			57	59	75	69	80	48	56	65	57	54	64	38	76	59
Sex			F	F	M	F	M	F	M	M	F	F	M	F	F	F
Time post onset (months)			77	96	73	101	24	48	144	264	100	108	54	70	29	11
Neuropsychological assessment																
Picture naming	64	59	**19**	**1**	61	**43**	**13/16***	**0**	**50**	**50**	**46**	**10/16***	**3**	62	**56**	**18/32***
Word-picture matching	64	62	**60**	63	62	63	15/16*	**61**	62	64	63	16/16	**52**	62	64	64
CCT_word	64	56	**29**	**39**	**43**	**48**	**49**	**50**	**52**	**53**	56	56	57	60	61	63
CCT_picture	64	52	**45**	**31**	**44**	**51**	**9/25***	59	57	56	61	57	54	61	53	58
Ambiguity nondominant	30	28	**14**	**11**	**9**	**18**	**21**	**17**	**17**	**14**	**21**	**22**	**19**	**19**	**21**	**23**
Object use task alternative	37	34	**14**	**14**	**13**	**27**	NT	**24**	**22**	**21**	**32**	NT	**22**	**29**	**26**	NT
Category fluency (mean)	-		5	0	7	4	7	0	7	4	15	9	0	17	17	0
Cookie theft (words-per-minute)	-		9	0	18	21	NT	0	37	12	38	29	0	37	54	0
PALPA Word repetition	16		12	0	14	11	15	0	16	15	6	15	2	16	15	2
Forward digit span	-	5	**2**	**0**	**4**	**3**	5	**0**	**4**	5	6	**3**	**0**	5	5	**4**
Raven's coloured matrices	36		31	31	29	31	21	32	30	24	33	22	34	33	21	32
Brixton (correct)	54	28	**18**	**21**	**7**	NT	**5**	**6**	**23**	**26**	39	36	31	30	31	39
Aphasia classification																
Fluency			Non-fl	Non-fl	Mid	Fluent	Mid	Non-fl	Fluent	Mid	Fluent	Fluent	Non-fl	Fluent	Fluent	Non-fl
Comprehension			Poor	Poor	Poor	Poor	Poor	Mid	Mid	Mid	Good	Good	Poor	Good	Good	Good
Repetition			Mid	Poor	Good	Mid	Good	Poor	Good	Good	Mid	Good	Poor	Good	Good	Poor
			Mixed TA	Global	TSA		TSA	Broca's	Anomic	Anomic	Anomic	Anomic	Global	Anomic	Anomic	Broca's

Normal cut-off = two s.d. below the control mean as reported by Jefferies & Lambon Ralph (2006). Scores in bold font are below the cut-off. CCT: Camel and Cactus test from Bozeat et al. (2000). PALPA = Psycholinguistic Assessment of Aphasia. Fluency classification is based on cookie theft scores: fluent > 20 words per minute; non-fluent < 10 words per minute. Comprehension classification is based on three pointing tasks from Cambridge semantic battery (word-picture matching;

CCT_word; CCT_picture). Repetition is based on PALPA word repetition : poor < 3; mid = 3-12 items correct. Non-fl = non-fluent. TA = transcortical aphasia. TSA = transcortical sensory aphasia. *Test was only partially completed

2.3 Lesion identification methods

Structural T1 images were obtained for all participants prior to the functional runs (3D FSPGR). A semi-automated method of lesion identification was used, whereby a rough lesion outline for each patient was drawn by hand using MRICron. The Clinical toolbox within SPM8 (Rorden et al., 2012) was then used to automate the lesion identification process within the prescribed area and to identify areas of lesion overlap. This method involved enantiomorphic normalization, which uses information from the contralateral intact hemisphere to 'fill in' the area marked by the lesion mask (Nachev et al., 2008). The primary area of damage for all patients was the posterior portion of the inferior frontal gyrus, extending into the precentral gyrus (peak overlap MNI = -38 16 15; lesion overlap map Figure S1). No patients showed any damage to the vATL. The pMTG region of interest (ROI) identified in this study was also intact in all patients.

2.4 Experimental materials

Materials were taken from the set of stimuli used by Rodd (2005). Sentences were selected that either contained a high or low degree of semantic ambiguity. Briefly (i) ambiguous sentences contained at least two ambiguous words which were either homonyms or homophones (e.g. the *creak* came from a *beam* in the ceiling), (ii) unambiguous sentences were matched to ambiguous sentences for number of words and syntactic structure. Unambiguous sentences were matched to ambiguous sentences for number of syllables (unambiguous = 8.64, ambiguous = 8.64), duration (mean length unambiguous = 2.01s, ambiguous = 2.03s), 'naturalness' rating (mean unambiguous = 6.49, ambiguous = 6.25), 'imageability' rating (unambiguous = 5.42, ambiguous = 5.58), and mean frequency of content words in the CELEX database (Baayern et al., 1995; unambiguous = 4.7, ambiguous = 4.5). (iii) Spectrally rotated speech (SRS; Blesser, 1972) was also created from these sentences, by spectrally inverting them using MATLAB (The MathWorks Inc., Natick, MA) scripts. SRS shares some spectrotemporal properties with unprocessed speech but it is unintelligible (Blesser, 1972, Scott et al., 2000).

2.5 Task fMRI acquisition

Whole-head fMRI data (Gradient echo, echo-planar imaging sequence, TR=2s, TE=minimum full, flip angle=90°) were acquired on a GE Signa HDx3T system (GE, Waukesha, WI, USA) using an eight-channel phased array head coil. A 64x64 matrix with a field of view of 19.2cm was used, giving an in-plane resolution of 3mm x 3mm. 28 interleaved slices were collected with a slice thickness of 3mm. The study used the MR sequence Interleaved Silent Steady State Imaging (ISSS; Schwarzbauer et al., 2006), which has been previously used to overcome some of the issues relating to scanner noise during auditory experiments (Rodd et al., 2012, Hymers et al., 2015). In brief, the method allows for a quiet period of several seconds in which auditory stimuli can be presented without accompanying background scanner noise, followed by the acquisition of several volumes following the offset of this period. This method is an alternative to traditional sparse imaging and has been shown to be more sensitive for auditory experiments (Mueller et al., 2011). The fMRI response in auditory cortex typically peaks about 4-5s after the presentation of an auditory stimulus (e.g. Hall et al., 2000) and therefore this sequence captures brain activity to an ongoing response that began prior to data acquisition. Stimuli were presented in three experimental runs. Each run consisted of the presentation of 8 ambiguous sentences, 8 unambiguous sentences, 8 SRS (4 of which were rotated versions of ambiguous sentences, 4 unambiguous sentences). Each sentence was presented in a 6-second quiet period. The 6-second quiet period was the same length for each stimulus; each sentence was presented so that there was 200ms in between the offset of the stimulus and onset of the acquisition of functional volumes. There were four stimulus acquisition volumes acquired after each trial, giving a trial of 14 seconds. Stimuli were presented in a pseudo-randomised order. 4 trials were also included in each block where no auditory stimulus was presented. Each run was therefore 6 mins 46 seconds and involved collection of 116 volumes.

To normalise variation in sound level across each sentence, stimuli were subject to dynamic range compression in Audacity (Audacity® version 2.0.3). All stimuli were normalised to -25 db FS. During the experiment participants wore earplugs, in addition to sound-attenuating fMRI-compatible headphones (MR Confon, MR Confon GmBH). Stimuli were presented using Presentation 13.1 (NBS

labs). Prior to the first experimental run participants were played three test sounds (two sentences and one SRS sentence, not used in the subsequent experimental runs) and all verified, either verbally or by button press, that they were able to hear the stimuli comfortably.

The paradigm was designed to be suitable for patients. To this end, participants in both patient and control groups were instructed to simply listen carefully to the sentences. A vigilance task was included in order to maintain participants' attention throughout the duration of each run; on a number of trials within each block, a visual cue of a picture of a finger pushing a button was presented in the volume acquisition period following offset of the stimulus. Participants were required to press a button with their left index finger using an MRI-compatible response box when they saw this image appear. The image appeared 3 times in a pseudorandomised order within each run. These trials were modelled separately within the brain imaging analysis. On the majority of trials where participants were not required to make a response, a simple fixation cross was presented. Prior to entering the scanner, all participants were also played three example stimuli (two sentences and one SRS, not used in the subsequent scanning session) to familiarise them with the nature of the stimuli.

2.6 Resting state fMRI acquisition

Resting state fMRI was collected on a separate day for 10 patients in the sample. We also collected resting state fMRI for 10 of the control participants. These data were acquired using the same scanner and coil as for the task experiment. Resting state data was acquired using a continuous GE-EPI sequence (TR=3s, TE=minimum full, flip angle=90°TR). A 64x64 matrix with a field of view of 19.2cm was used, giving an in-plane resolution of 3mm x 3mm. 60 interleaved slices were collected with a slice thickness of 3mm. The scan duration was 9 min giving a total of 180 volumes of data. During the resting state scan participants were instructed to maintain fixation on a black fixation cross on a grey background.

The analyses below also make use of a large set of resting state scans to characterize the normal functional connectivity of the site of maximal lesion overlap. For this analysis we utilised a publically available data set of 141

participants (Cohort 4, Mean Age = 37, SD = 13.9, 102 females) from the Nathan Kline Institute (NKI; Nooner et al., 2012; see Gorgolewski et al. (2014). Parameters of the independent (NKI)/Rockland Enhanced Sample are described in detail by Gorgolewski et al. (2014) and Smallwood et al. (2016). The size of this sample allowed us to reliably characterize the intrinsic connectivity of the lesion site, in general terms; for this reason, the NKI sample was considered preferable to the more limited resting-state fMRI data from our own control participants.

2.7 Task fMRI pre-processing and analysis

Data were pre-processed in FSL v4.1, using Feat-5.98 (part of FMRIB Software library) in addition to custom scripts that allowed for temporal filtering of the non-contiguous data. At the first level, a separate analysis was carried out for each participant. Data were motion corrected with MCFLIRT (Jenkinson et al., 2002) and enantiomorphically normalised brains were brain extracted using BET (Smith, 2002). EPI data were smoothed with a Gaussian kernel of 8mm FWHM. Custom scripts also removed linear and quadratic trends per-voxel, taking into account the times at which data were acquired.

Each condition (ambiguous, unambiguous or SRS) was modelled as a separate explanatory variable (EV). The design matrix was conducted in a similar fashion to that described in Hymers et al. (2015). Briefly, the design matrix was initially constructed in accordance with the overall length of the experiment. Each event in the design matrix was modelled as the 2 second period following offset of the stimulus, and was convolved using the double gamma HRF and its temporal derivative (Friston et al., 1998). The design matrix was then resampled to reflect the time at which the volume acquisition occurred using in house scripts (available on request, Hymers et al., 2015). The six motion correction parameters were included in the model. All regressor heights for each EV and contrast were recalculated in accordance with the resampled design matrix. Beta values were then estimated by using FMRIB's Improved Linear Model (FILM) and parameter estimates for each condition (unambiguous, ambiguous, and SRS) were pooled. A second level, within-subjects, fixed effects analysis combined parameter estimates together for each of the 3 runs. This was then taken forward to a group level mixed

effects analysis using FLAME (FMRIB's Local Analysis of Mixed Effects; Beckmann et al., 2003, Woolrich et al., 2004) stage 1.

We first conducted whole-brain analyses of the task data within a semantic mask to characterize sentence processing in the two groups. The binary mask that was obtained using the online meta-analytic search tool *Neurosynth* (Yarkoni et al., 2011; search term: "semantic"; 844 contributing studies; reverse inference, www.neurosynth.org/analyses/terms/) and corresponded to brain regions already implicated in semantic processing across studies. This mask was used to restrict the analysis to areas that are plausible candidates for supporting residual comprehension in patients with SA, since we had relatively few participants in each group. Data were thresholded at z=1.96 (i.e. p=.05) with a cluster significance threshold of p<.05 FWE corrected. We conducted further ROI analyses to investigate the neural response to the ambiguous and unambiguous sentences in ATL and pMTG, given our strong a priori hypothesis that these regions will contribute to functional compensation following LIFG damage. Spherical ROIs with 5mm radius were centred on (i) a peak in pMTG that showed a strong response to diverse manipulations of semantic control in a meta-analysis of neuroimaging studies (Noonan et al., 2013; coordinates: MNI -45 19 21) and (ii) a site in ventral ATL thought to support the computation of coherent heteromodal concepts, taken from Binney et al., 2010 (coordinates: MNI -39 -9 -36).

Given that co-registration and normalization of lesioned brains can be problematic (see Crinion et al., 2007, Nachev et al., 2008), we manually checked that the ROIs for the patients corresponded to the relevant region of cortex in each individual brain by back-transforming the spherical ROI to native space using ApplyXFM within FSL. For these ROIs, percent signal change was extracted using FEAT query within FSL, and these values were entered into a 2 X 2 x 2 ANOVA to investigate the main effects of site, group and condition, and their interactions. One sample t-tests were used to investigate whether the signal change in each condition for each ROI was significant.

2.8 Resting state pre-processing and analysis

Resting state data were analysed in FSL v4.1, using Feat-5.98 (part of FMRIB Software library). Structural T1 weighted images were brain extracted

using BET and these scans were registered to standard space using FLIRT (Jenkinson & Smith, 2001). Prior to conducting the functional connectivity analysis the following pre-statistics processing was applied to the resting state data; motion correction using MCFLIRT (Jenkinson, Bannister et al. 2002); slice-timing correction using Fourier-space time-series phase shifting; non-brain removal using BET (Smith 2002); spatial smoothing using a Gaussian kernel of FWHM 6mm; grand-mean intensity normalization of the entire 4D dataset by a single multiplicative factor; high pass temporal filtering (Gaussian-weighted least-squares straight line fitting, with sigma = 100 s); Gaussian low pass temporal filtering, with sigma= 2.8 s.

Spherical seed ROIs with 3mm radius were constructed for the ROIs in vATL and pMTG. The time-series of these regions were extracted and used as explanatory variables in a separate subject-level functional connectivity analysis for each seed. In these analyses, we also included 11 nuisance regressors: the top five principal components extracted from white matter (WM) and cerebrospinal fluid (CSF) masks in accordance with the CompCor method (Behzadi, Restom et al. 2007) and six motion parameters. The WM and CSF masks were generated by segmenting each individual's high-resolution structural image (using FAST in FSL). The default tissue probability maps, referred to as Prior Probability Maps (PPM), were registered to each individual's high-resolution structural image (T1 space) and the overlap between these PPM and the corresponding CSF and WM maps was identified. Finally, these maps were thresholded (40% for the CSF and 66% for the WM), binarized and combined. The six motion parameters were calculated in the motion-correction step during pre-processing. No global signal regression was performed (Murphy, Birn et al. 2009).

2.9 Signal-to-noise ratio in the ROIs

To assess whether our ROIs had sufficient signal to detect reliable activation (given the possibility of signal dropout within the more ventral aspect of the ATL), we calculated the temporal signal-to-noise ratio (tSNR) for the first run of the experiment for each participant. This was performed in the manner described by Friedman et al. (2006) by dividing the mean signal in each voxel by the standard deviation of that voxel's residual error time series. The resulting

value was then averaged across all voxels within the ROI. We calculated the tSNR for the vATL and pMTG ROI for patients and controls, in the task data and in the resting state scan. Mean tSNR values across participants in the task data were: vATL ROI = 47.07, pMTG ROI = 74.64; resting state data: vATL ROI = 51.73, pMTG ROI = 75.37. The percentage of voxels with 'good' tSNR values of above 20 (as outlined in Binder et al., 2011) was as follows: task data: vATL ROI = 98%, pMTG ROI = 100%; resting state data: vATL ROI = 96.6%, pMTG ROI = 100%. This indicates that although tSNR was lower in the vATL, as has been widely reported previously (Binney, Hoffman & Lambon Ralph, 2016, Devlin et al., 2000, Visser et al., 2010), the tSNR was still at an acceptable level to detect reliable fMRI activation (Binder et al., 2011).

3.0 Results

The analyses presented below followed the following steps: (i) We identified a site lesioned in all patients in left inferior frontal cortex. (ii) We established that this site showed a pattern of strong intrinsic connectivity with other regions implicated in semantic control in non-lesioned brains. (iii) We identified sites activated by the sentence listening paradigm that lay outside the lesioned area. These sites included two ROIs thought to be candidates for supporting residual comprehension in patients with damage to left inferior frontal cortex; namely pMTG and vATL. (iv) We characterized the intrinsic connectivity of these ROIs in the patient and control groups, to establish whether these sites formed a functional network with the damaged left inferior frontal cortex. (v) We extracted the percentage signal change for each condition of the sentence listening paradigm for these ROIs in each group, to determine how damage to left inferior frontal cortex influenced the level of functional recruitment within these sites. (vi) We related this functional recruitment across participants to levels of intrinsic connectivity for these sites, to investigate how changes in recruitment might be reflected in the functional organization of the semantic system measured at rest. (vii) Finally, we examined whether these patterns of connectivity related in a positive or negative fashion to semantic performance measured outside the scanner.

All maps generated in this study are freely available at the following URL at Neurovault: http://neurovault.org/collections/2221/

3.1 Functional connectivity of the lesion site

Our first analysis was to use resting-state fMRI data to examine whether the site of maximal lesion overlap was part of a functional network that included the pMTG and vATL ROIs. All of the SA patients included in this study had some damage to left inferior frontal cortex, and the site of maximum lesion overlap was at the boundary of posterior LIFG and precentral gyrus (see left-hand column of Figure 2). We investigated this location of maximal lesion overlap by placing a sphere in the grey matter adjacent to the peak lesion overlap (seed region in left-hand column, damaged in all fourteen patients; MNI coordinates = -45 7 10). We then characterized the intrinsic connectivity of this sphere in a large sample of resting-state fMRI data from healthy individuals (NKI sample; see Methods). The results in the middle two columns of Figure 2 show that the site of maximal lesion overlap is functionally coupled with both pMTG and vATL in the left hemisphere. To quantify the overlap between this functional connectivity map and regions implicated in semantic control, we overlaid this map with the meta-analytic map of semantic control produced by Noonan and colleagues (2013). There was a high degree of overlap between these spatial maps (bottom right in Figure 2). Thus our ROIs in vATL and pMTG participate in a large-scale network that includes the site damaged in the majority of the patients. Table S1 in the Supplementary materials presents the full details of the spatial map produced through this analysis.

Figure 2: Functional connectivity pattern for the site of maximal lesion overlap

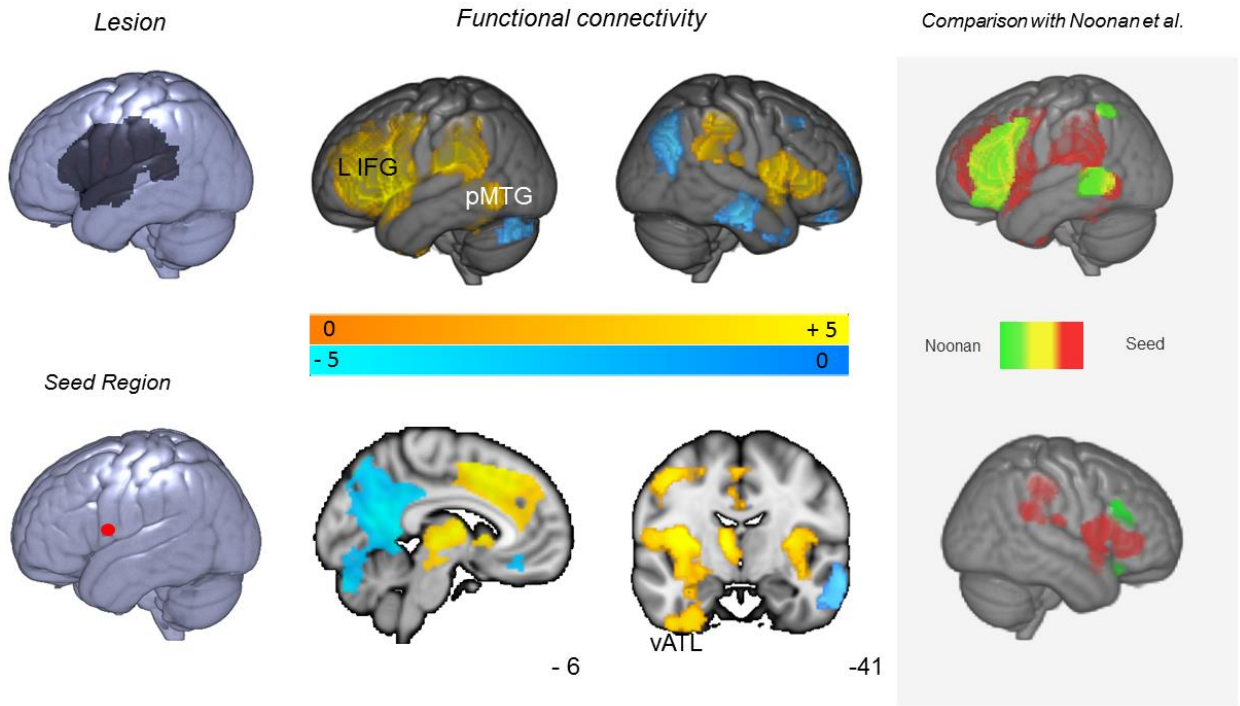

The top left of this figure shows the lesion overlap map for the patient group. This lesion map is thresholded at minimum of 7 patients who showed overlapping damage. All patients in the sample showed a lesion overlap at the boundary of posterior LIFG and precentral gyrus (bottom left). We seeded this peak overlap location in an independent dataset (NKI) to reveal the intrinsic connectivity at rest of the network commonly damaged in the patients (middle two columns). This pattern of connectivity overlapped with regions known to be involved in semantic control (right-hand column; from Noonan et al., 2013).

3.2 Neural processing associated with sentence comprehension

We next considered the neural activation associated with sentence processing in patients and controls. We used a mask that restricted the scope of our search to regions identified as important for "semantics" using Neurosynth (see Methods). Neural activation within this mask associated with attending to meaningful speech relative to unintelligible SRS was seen within multiple left hemisphere sites, including anterior temporal lobes (ATL), both vATL and aSTG, plus pMTG and LIFG in both patients and controls (see Figure 3, top row). The majority of the LIFG cluster was outside the area of lesion. This analysis demonstrates that the sentence listening task successfully activated regions

important for semantic processing in both groups, including sites of interest in vATL and pMTG – which, in the analyses that follow, are taken forward as ROIs. Table S2 in the Supplementary Materials presents the full details of the spatial map produced through this analysis.

Figure 3: Task-based activation and seeding of regions of interest in the resting-state

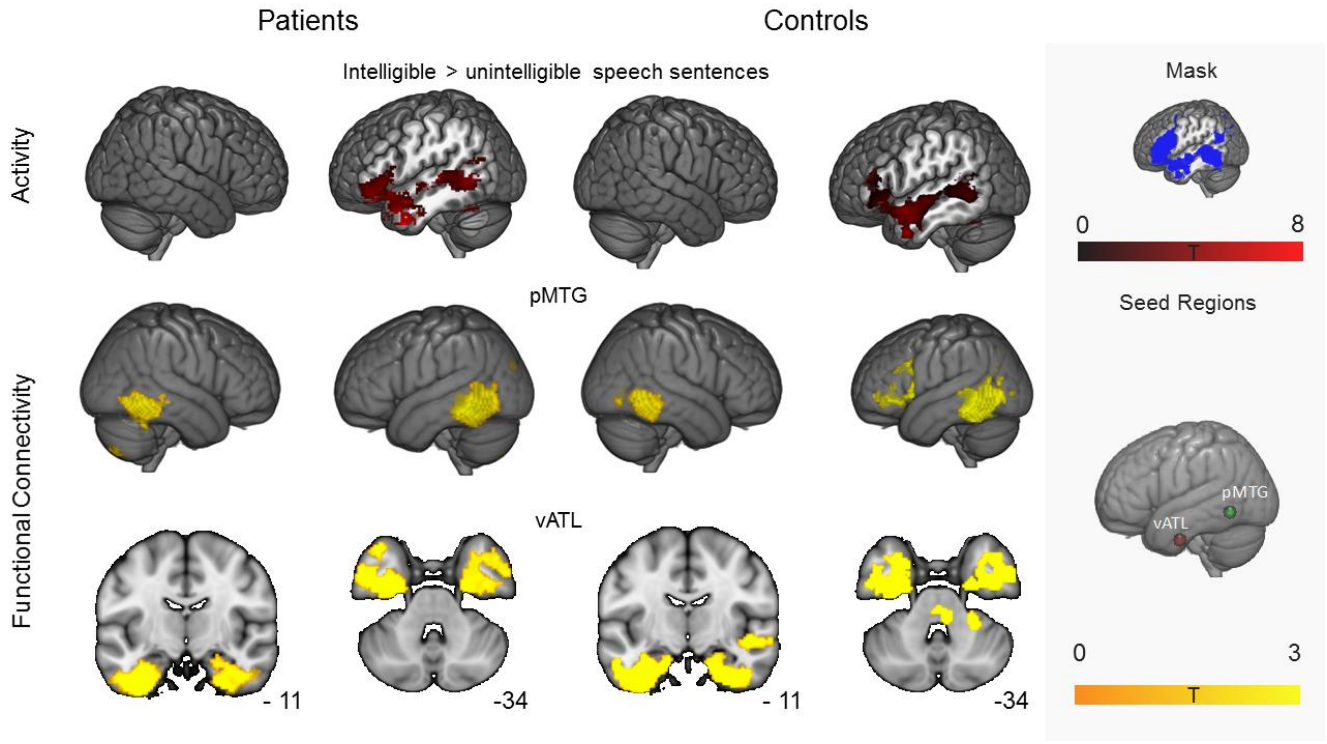

Activation for the contrast of sentences > noise for patients and controls, identifying a bilateral network including anterior temporal lobes (ATL), posterior middle temporal gyrus (pMTG) and left ventral inferior frontal gyrus (IFG) in both groups. These maps are masked by areas involved in semantic processing identified using Neurosynth. The bottom two rows shows common areas of connectivity when seeding from two key sites activated by these contrasts and largely undamaged in the patient group (pMTG and vATL).

3.3 Functional connectivity of the nodes of the semantic system in patients and controls at rest

The analysis above demonstrates that both groups showed activation in the sentence listening task in undamaged parts of the semantic network, including two regions of interest thought to be candidates for supporting comprehension

following damage to LIFG; namely a second site implicated in semantic control in addition to LIFG (pMTG) and a region thought to support multimodal conceptual representation (vATL). The lower two rows of Figure 3 presents the functional connectivity associated with these two ROIs, taken from a meta-analysis of semantic control tasks by Noonan et al. (2013; pMTG -57 -54 -9) and from a study of semantic processing designed to optimise signal in vATL by Binney et al. (2010; vATL -39 -9 -36). These maps reflect the connectivity pattern for spheres placed around relevant coordinates from the literature, which fell within the area of activation during sentence listening in both groups. In controls, the left pMTG was functionally connected to LIFG as well as right pMTG. In the patients we observed a similar pattern, except the connection to LIFG was absent, likely reflecting structural disconnection between the two sites caused by damage within and beyond LIFG. The vATL had a more restricted pattern of connectivity, limited to its right hemisphere homolog. There were no clear differences in the functional connectivity of vATL between patients and controls. Table S3 in the Supplementary Materials presents the full details of the spatial map produced through this analysis.

3.4 Regions of interest analysis on processing the semantic ambiguity within sentences

To characterize the response to the sentence listening task in the regions of interest in pMTG and vATL, we extracted the percent signal change for ambiguous and non-ambiguous sentences, for patients and controls, within these spherical ROIs (Figure 4 and 5). We calculated the difference in signal for ambiguous and non-ambiguous sentences over SRS sentences, and examined the within-participant factor of ambiguity (High / Low) and the between-participant factor of group (Patients / Controls) using ANOVA. We observed a main effect of group, reflecting a higher response to sentences in the patients than controls ($F(1,28) = 7.23$, $p < .05$). There was also a main effect of site (stronger signal within pMTG than vATL; $F(1,28) = 6.49$, $p = .017$) and a main effect of ambiguity, indicating a stronger response to ambiguous sentences ($F(1,28) = 12.10$, $p = .002$). Other effects were non-significant.

3.5 Relationship between the nodes of the semantic system during tasks and at rest

Having determined how pMTG and vATL responded to the sentences in the patients and controls, as well the intrinsic functional connectivity of these sites at rest, our next analyses considered the relationship between these regions' behaviour in tasks and at rest.

pMTG: This site showed a stronger response to the sentence listening task in the patients than the controls ($F(1,28) = 6.146$, $p < .05$), an effect of ambiguity that approached significance ($F(1,28) = 4.121$, $p = .052$) and no interaction between group and ambiguity ($F(1,28) = 1.492$, $p = .232$). We included the difference in activity during ambiguous and non-ambiguous sentences in the pMTG ROI as an explanatory variable in a group-level regression of resting-state functional connectivity, to identify regions where the strength of functional connectivity at rest from pMTG was associated with the magnitude of the ambiguity effect in the task. This revealed a functional activation by group interaction in a region of anterior superior temporal gyrus (aSTG) extending into the most ventral aspects of inferior frontal gyrus (see Figure 4 and Supplementary Table S4); i.e., the connectivity between this region and pMTG varied according to ambiguity in a different way across the two groups. To understand this pattern in greater detail, we extracted the connectivity from within this mask and plotted it against the percentage signal change reflecting the ambiguity effect in each group. For controls, strong activity in pMTG for ambiguous relative to non-ambiguous sentences was associated with *reduced* functional connectivity to aSTG [$r = -.823$, $p < .01$], but this relationship was reversed in SA patients who showed *stronger* functional coupling with this region [$r = .758$, $p < .05$].

Finally, we considered the functional significance of this effect by relating the strength of pMTG-aSTG connectivity to semantic performance measured outside the scanner in the patient group. We examined a verbal association task (Camel and Cactus Test presented as words), for which we had behavioural measurements on the same task for every case, and found that stronger coupling between pMTG and aSTG predicted better patient performance [$r = .653$, $p < .05$]. Thus, functional connectivity between the pMTG and aSTG was higher for

individuals with aphasia whose semantic cognition was relatively preserved following a stroke affecting left prefrontal cortex. We also examined the correlation with the ambiguity task but found no significant correlation with the dominant (r = .186, p = .63) or non-dominant (r = .188, p = .628) conditions of the task.

Figure 4: Regions that show changes in intrinsic connectivity at rest as a function of task activation for ambiguous versus unambiguous sentences in pMTG.

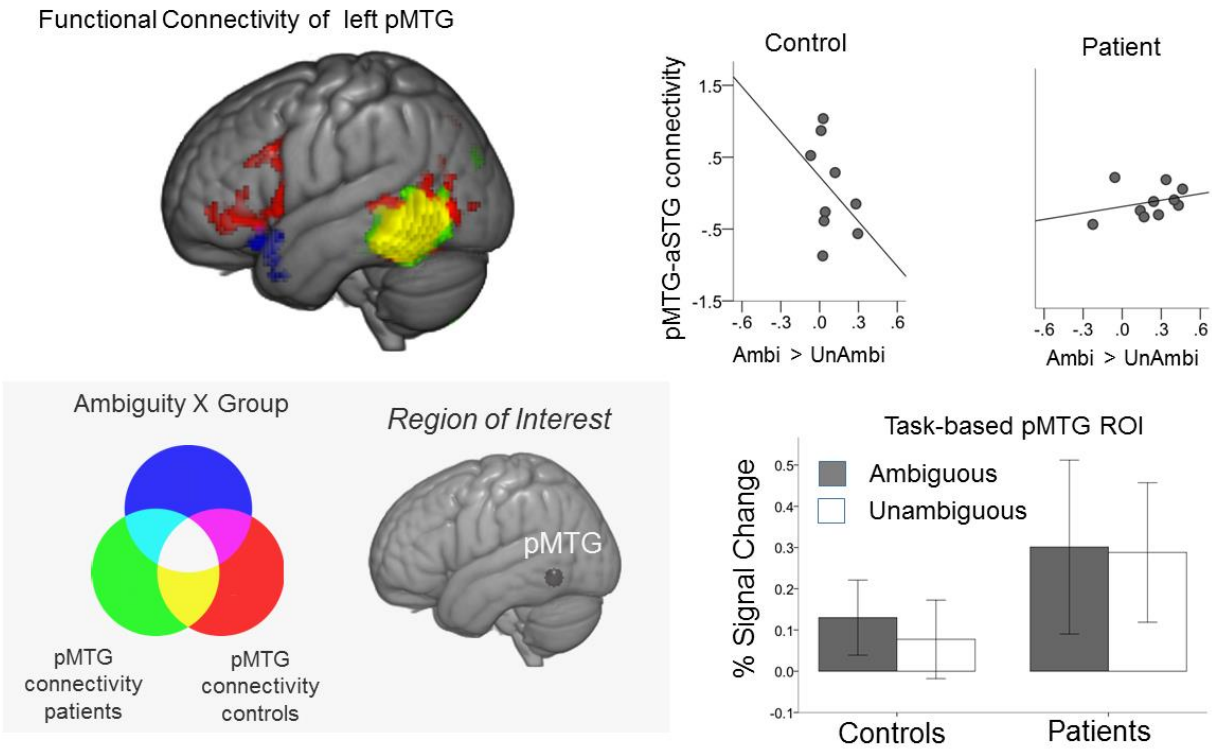

Group level regression examining regions that show changes in intrinsic connectivity at rest as a function of task activation for ambiguous over unambiguous sentences in the pMTG ROI. Scatter plots show connectivity from within the resulting mask against the ambiguity effect in the seed region in each group. For controls, activation in pMTG for ambiguous over unambiguous sentences was associated with reduced functional connectivity to a region in anterior Superior Temporal Gyrus (aSTG) in the left temporal lobe [r = -.823, p<.01], but this relationship was reversed in SA patients who showed stronger functional coupling with this region [r = .758, p<.05].

vATL: Like pMTG, this site showed a stronger response to the sentence listening task in the patients than the controls ($F(1,28) = 4.840$, $p < .05$), but only

a weak and non-significant effect of ambiguity ($F(1,28) = 3.377$, $p = .077$) and no interaction between these factors ($F(1,28) = .003$, $p = .954$). Examination of the relationship between the behaviour of vATL during tasks and rest revealed that, regardless of group, there was stronger connectivity between the ROI in vATL and a region of ventral LIFG for participants who showed stronger recruitment of the ROI for ambiguous over unambiguous sentences (see Figure 5). To understand this pattern in greater detail, we extracted the connectivity from within this mask (the mask included only areas that were undamaged in all of the patients) and plotted it against the percentage signal change reflecting the difference in recruitment between ambiguous and non-ambiguous sentences. This confirmed that in both SA patients [$r = .636$, $p<.05$] and controls [$R=.716$, $p<.05$], greater recruitment of vATL during the processing of ambiguous sentences was associated with greater functional connectivity of this region with ventral LIFG. Unlike pMTG, there was no relationship between this pattern of connectivity and performance on the verbal Camel and Cactus Task ($r=-.415$, $p=.232$) or on the dominant ($r=-.247$, $p=.521$) or non-dominant ($r=-.266$, $p=.490$) conditions of the ambiguity task.

Figure 5: Regions that show changes in intrinsic connectivity at rest as a function of task activation for ambiguous over unambiguous sentences in vATL

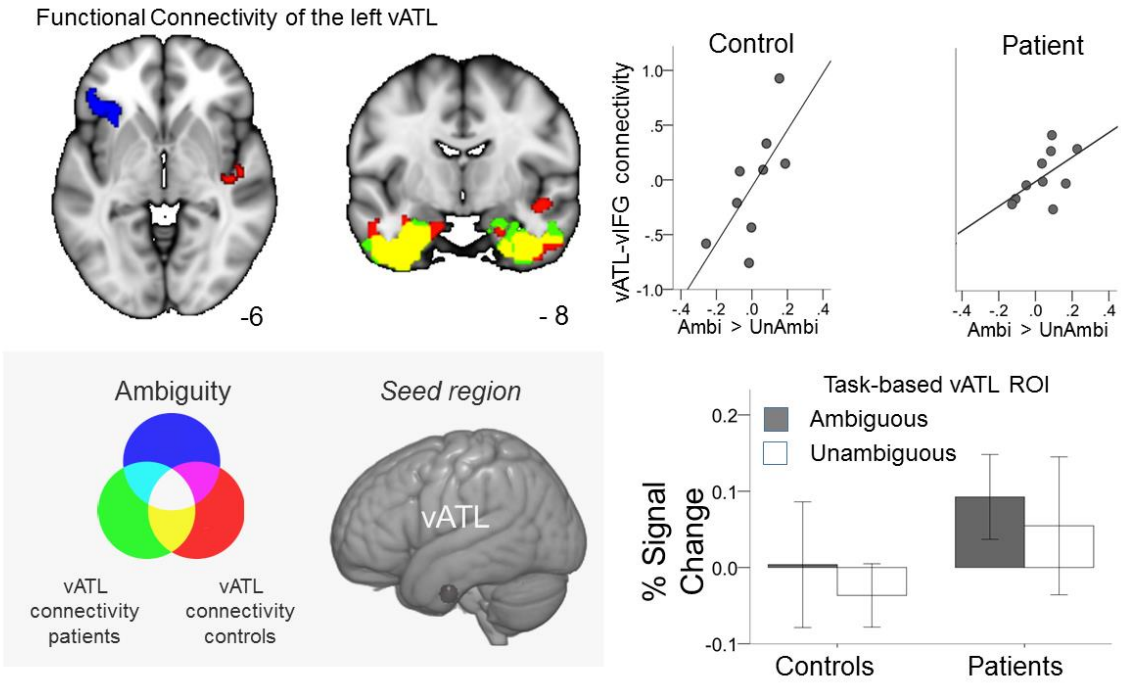

Group level regression examining regions that show changes in intrinsic connectivity at rest as a function of task activation for ambiguous over unambiguous sentences in vATL. In both SA patients [r = .636, p<.05] and controls [R=.716, p<.05], greater recruitment of vATL for ambiguous items was associated with greater functional connectivity between this region and ventral inferior frontal gyrus (outside the lesioned area).

4.0 Discussion

Over the last decade, numerous studies have shown that semantic deficits in aphasia can reflect deficient control over conceptual retrieval (Jefferies & Lambon Ralph, 2006, Thompson et al., 2015, Corbett et al., 2011., Noonan et al., 2010, Jefferies, 2013), but the neural basis of this type of semantic impairment has hardly been explored. This study examined neural recruitment in patients with poor control over semantic retrieval during a sentence listening task using sentences that varied in their levels of ambiguity. We used a combination of (i) task-based fMRI and a sparse imaging sequence that allowed us to characterize the processing of meaningful speech in both groups, plus (ii) task-free resting-state methods to assess the connectivity of the semantic system. This multi-

method approach was used to establish how neural recruitment during comprehension changes in patients with semantic control deficits, and how this recruitment is linked to the functional architecture of the semantic system at rest.

Every patient in our sample showed deficient semantic control associated with damage to left posterior inferior prefrontal cortex. This region is thought to play a critical role in semantic control across tasks and modalities (Thompson-Schill et al., 1997, Badre et al., 2005, Noonan et al., 2013, Whitney et al., 2011), and in line with this characterization, the patients were unable to retrieve less dominant aspects of meaning in both verbal and picture-based tasks. Comparison of the commonly-lesioned areas in this sample (in left prefrontal and superior temporal cortex) with a meta-analytic map of semantic processing from Neurosynth identified two regions critical to semantic cognition that were largely undamaged in our patients. These sites were in vATL (implicated in semantic representation; Patterson et al., 2007, Lambon Ralph et al., 2010, Rogers et al., 2004, Pobric et al., 2010., Lambon Ralph et al., 2017) and pMTG (thought to co-activate with LIFG as part of a distributed network underpinning semantic control; Hallam et al., 2016, Hoffman et al., 2010, Noonan et al., 2013, Davey et al., 2015, Whitney et al., 2011., Gold et al., 2006, Davey et al., 2016). We examined the response of these regions-of-interest, and found that patients recruited them both to a greater extent than the controls. This is consistent with the possibility that comprehension in patients with LIFG lesions relies more on activation within pMTG and vATL – i.e., that these regions help to compensate for damage to LIFG. Alternatively, given that there was a main effect of group and a near-significant effect of ambiguity in the BOLD response in both ROIs, this greater response could conceivably have reflected the effort required to process the sentences.

In order to understand more about the functional contribution of this increased response in pMTG and vATL, we examined the relationship between the functional recruitment of these regions in sentence comprehension and their intrinsic connectivity at rest. For controls, heightened activation of pMTG in response to ambiguous sentences was associated with reduced correlation at rest with LIFG, a site commonly implicated in semantic control (Badre et al., 2005; Noonan et al.,

2013; Whitney et al., 2011), as well as weaker coupling with anterior STG. In contrast, a positive correlation between pMTG and aSTG was observed for the SA patients – and the magnitude of this positive coupling predicted better performance on the Camel and Cactus test of verbal association, consistent with the hypothesis that the response in pMTG supports semantic cognition in the face of LIFG damage. Functional neuroimaging studies of healthy participants have suggested that aSTG has a different functional profile from vATL: rather than showing a multimodal semantic response across verbal and non-verbal tasks, this region is specifically recruited during auditory-verbal semantic processing (Murphy et al., 2017). Anterior STG also shows a different pattern of intrinsic functional connectivity from vATL, with stronger coupling with auditory-motor regions, and weaker connectivity with the default mode network and heteromodal semantic areas (Jackson et al., 2016, Murphy et al., 2017). Consequently, relatively good verbal comprehension in patients with SA was related to stronger connectivity between a posterior semantic control site (pMTG) and a region associated with verbal semantic processing (aSTG).

Increased functional connectivity in the patient sample relative to controls might be expected to be restricted to regions that support *controlled* semantic retrieval, e.g., pMTG (Davey et al., 2016). In line with this proposal, increased functional recruitment during the processing of ambiguous speech in vATL was associated with increased functional coupling with a region of ventral LIFG at rest for both patients *and* controls. This ventral LIFG region was largely outside the lesion area in the patient group. Thus, we found an abnormal pattern of functional connectivity from a non-damaged region within the semantic control network (pMTG), but a normal pattern for the putative semantic store in vATL. These findings fit well with theoretical accounts of SA that emphasise the preservation of semantic knowledge in an amodal conceptual 'hub' in vATL (which captures meaning in concert with modality-specific representations in "spoke" regions; Patterson et al., 2007, Lambon Ralph et al., 2017). Comprehension deficits that arise from damage to left IFG are instead thought to reflect difficulty constraining the retrieval of semantic representations in a task-relevant manner, and these

problems might benefit from engagement of another region in the semantic control network.

Our findings have important theoretical implications for understanding how semantic control is implemented by the cortex. Converging evidence from neuropsychology, neuroimaging and transcranial magnetic stimulation highlights the role of a left lateralized functional network including both left IFG and pMTG in constraining semantic processing to suit the demands of a task or context (Jefferies, 2013). In this regard, our study shows that, at rest, aberrant functional behaviour in pMTG, but not vATL, emerges from lesions that are primarily focused in left prefrontal cortex. This dissociation can be easily accounted for by the hypothesis that left IFG and pMTG work in tandem to flexibly constrain semantic processing to fit into the momentary demands posed by a task (Jefferies, 2013; Whitney et al., 2011, Noonan et al., 2013). When one site within the distributed system underpinning semantic control is damaged (left prefrontal cortex), the ability to understand words is linked to the capacity to activate and connect a second site, the pMTG, within the semantic control network. Similar findings were recently observed in a study using TMS to disrupt the normal functioning of LIFG in healthy volunteers (Hallam et al., 2016). Augmenting this compensatory response in pMTG is a clear target for speech and language therapy in patients with comprehension deficits resulting from poor control over retrieval in aphasia.

It is worth noting some limitations of the study. One issue relates to the use of the ISSS sequence: this was selected as it was optimal for characterizing activation in response to the auditory sentences, but it made task-based connectivity difficult to assess. For this reason, we correlated task-based activation with intrinsic rather than task-based connectivity. A paradigm that used a more standard EPI sequence, as in Jackson et al. (2016), would have allowed us to consider similarities and differences in task-based and resting-state connectivity.

Secondly, in addition to deficits of semantic control, many of the patient volunteers in this study showed poor performance on non-verbal tests of executive function. This pattern replicates the findings of Jefferies & Lambon

Ralph (2006), who reported a correlation between semantic and non-semantic control deficits in patients with SA, in contrast to those with semantic dementia. This pattern is predicted by neuroimaging studies of healthy participants showing partially-overlapping and adjacent networks supporting semantic and domain-general executive control (e.g., Noonan et al., 2013). Difficult tasks across domains elicit activation within a multiple-demand network, including inferior frontal sulcus, intraparietal sulcus and pre-supplementary motor area (e.g., Duncan, 2010). Semantic control manipulations activate these regions in addition to more ventral and anterior parts of LIFG and pMTG, which lie outside the multiple-demand network (Noonan et al., 2013; Davey et al., 2016). Both the semantic control and the multiple-demand networks could have been affected in our patients (although the intrinsic connectivity of the peak lesion location at rest overlapped substantially with regions important for semantic control, while some sites strongly implicated in executive control – namely intraparietal sulcus – were not part of the network). Our findings do not preclude the possibility that patients might also show abnormal patterns of functional recruitment and connectivity in non-semantic tasks (e.g. Brownsett et al., 2014; Geranmayeh et al., 2014 although the focus of the current study was on characterizing the neural basis of residual comprehension following damage to left inferior frontal cortex.

Secondly, we opted to characterize the brain's response during passive listening to ambiguous and non-ambiguous sentences, since this precluded the possibility that the patients would show abnormal activation from a failure to understand the task instructions. There are likely to be differences in the neural response to semantic processing for single words compared with sentences (such as semantic combination processes; e.g. Price et al., 2015). However, previous studies examining the effects of ambiguity in auditory sentences (Rodd et al., 2005; 2012; 2015) identified regions of the semantic control network, such as LIFG and pMTG, which overlapped directly with areas implicated in semantic control in a meta-analysis of neuroimaging studies that used a wide range of task manipulations (Noonan et al., 2013). These included single word matching tasks varying the strength or number of distractors or the strength of the semantic link between the items. Ambiguous sentences might elicit a stronger response in semantic control

regions because, in common with other semantic control tasks, they require retrieval to be focussed on non-dominant aspects of knowledge as well as selection of appropriate representations from competing alternatives (Badre et al., 2005; Thompson-Schill et al., 1997). Indeed, Noonan et al. (2013) found that the type of comprehension task did not have a strong influence on recruitment across the semantic control network, presumably because all of these tasks shared the requirement to shape retrieval away from dominant patterns within long-term memory and towards alternative aspects of knowledge suitable for the current task goal or context. This observation can explain why abnormal recruitment and connectivity derived from a sentence listening paradigm predicted performance on more standard semantic assessments in patients with SA.

5.0 Acknowledgements

We thank the patients and their carers for their generous assistance with this study. GH was supported by a Stroke Association project grant (TSA/12/02). EJ was supported by grants from BBSRC (BB/J006963/1) and the European Research Council (SEMBIND – 283530), JS was supported by European Research Council (WANDERINGMINDS – 646927) and M.A.L by an MRC programme grant (MR/J004146/1). Funders had no role in study design, collection, analysis and interpretation of data, writing the report, or decision to submit the article for publication.

6.0 References

Adlam, A.-L. R., Patterson, K., Bozeat, S., & Hodges, J. R. (2010). The Cambridge Semantic Memory Test Battery: Detection of semantic deficits in semantic dementia and Alzheimer's disease. *Neurocase*, *16*(3), 193–207. https://doi.org/10.1080/13554790903405693

Baayen, R, R Piepenbrock, and L Gulikers. CELEX2 LDC96L14. Web Download. Philadelphia: Linguistic Data Consortium, 1995.

Badre, D., Poldrack, R. A., Paré-Blagoev, E. J., Insler, R. Z., & Wagner, A. D. (2005). Dissociable controlled retrieval and generalized selection mechanisms in ventrolateral prefrontal cortex. *Neuron*, *47*(6), 907–918. https://doi.org/10.1016/j.neuron.2005.07.023

Beckmann, C. F., Jenkinson, M., & Smith, S. M. (2003). General multilevel linear modeling for group analysis in FMRI. *NeuroImage*, *20*(2), 1052–63. https://doi.org/10.1016/S1053-8119(03)00435-X

Behzadi, Y., Restom, K., Liau, J., & Liu, T. T. (2007). A component based noise correction method (CompCor) for BOLD and perfusion based fMRI. *NeuroImage*, *37*(1), 90–101. https://doi.org/10.1016/j.neuroimage.2007.04.042

Berthier, M. L. (2001). Unexpected brain-language relationships in aphasia: Evidence from transcortical sensory aphasia associated with frontal lobe lesions. *Aphasiology*, *15*(2), 99–130. https://doi.org/10.1080/02687040042000179

Binder, J. R., Gross, W. L., Allendorfer, J. B., Bonilha, L., Chapin, J., Edwards, J. C., … Weaver, K. E. (2011). Mapping anterior temporal lobe language areas with fMRI: A multicenter normative study. NeuroImage. https://doi.org/10.1016/j.neuroimage.2010.09.048

Binney, R. J., Embleton, K. V., Jefferies, E., Parker, G. J. M., & Lambon Ralph, M. A. (2010). The Ventral and Inferolateral Aspects of the Anterior Temporal Lobe Are Crucial in Semantic Memory: Evidence from a Novel Direct Comparison of Distortion-Corrected fMRI, rTMS, and Semantic Dementia. Cerebral Cortex, 20(11), 2728–2738. https://doi.org/10.1093/cercor/bhq019

Binney, R. J., Hoffman, P., & Lambon Ralph, M. A. (2016). Mapping the Multiple Graded Contributions of the Anterior Temporal Lobe Representational Hub to Abstract and Social Concepts: Evidence from Distortion-corrected fMRI. *Cerebral Cortex*. https://doi.org/10.1093/cercor/bhw260

Blesser, B. (1972). Speech Perception Under Conditions of Spectral Transformation: I. Phonetic Characteristics. *Journal of Speech Language and Hearing Research*, *15*(1), 5. https://doi.org/10.1044/jshr.1501.05

Bozeat, S., Lambon Ralph, M. a., Patterson, K., Garrard, P., & Hodges, J. R. (2000). Non-verbal semantic impairment in semantic dementia. *Neuropsychologia*, *38*(9), 1207–1215. https://doi.org/10.1016/S0028-3932(00)00034-8

Brownsett, S. L. E., Warren, J. E., Geranmayeh, F., Woodhead, Z., Leech, R., & Wise, R. J. S. (2014). Cognitive control and its impact on recovery from aphasic stroke. Brain. https://doi.org/10.1093/brain/awt289

Burgess PW, Shallice T. The Hayling and Brixton tests. Bury St Edmunds: Thames Valley Test Company; 1997.

Corbett, F., Jefferies, E., & Ralph, M. a L. (2011). Deregulated semantic cognition follows prefrontal and temporo-parietal damage: evidence from the impact of task constraint on nonverbal object use. *Journal of Cognitive Neuroscience*, *23*(5), 1125–1135. https://doi.org/10.1162/jocn.2010.21539

Crinion, J., Ashburner, J., Leff, A., Brett, M., Price, C., & Friston, K. (2007). Spatial normalization of lesioned brains: Performance evaluation and impact on fMRI analyses. NeuroImage. https://doi.org/10.1016/j.neuroimage.2007.04.065

Davey, J., Cornelissen, P. L., Thompson, H. E., Sonkusare, S., Hallam, G., Smallwood, J., & Jefferies, E. (2015). Automatic and Controlled Semantic Retrieval: TMS Reveals Distinct Contributions of Posterior Middle Temporal Gyrus and Angular Gyrus. *Journal of Neuroscience*, *35*(46), 15230–15239.

Davey, J., Rueschemeyer, S.-A., Costigan, A., Murphy, N., Krieger-Redwood, K., Hallam, G., & Jefferies, E. (2015). Shared neural processes support semantic control and action understanding. *Brain and Language*, *142*, 24–35. https://doi.org/10.1016/j.bandl.2015.01.002

Davey, J., Thompson, H. E., Hallam, G., Karapanagiotidis, T., Murphy, C., De Caso, I., … Jefferies, E. (2016). Exploring the role of the posterior middle temporal gyrus in semantic cognition: Integration of anterior temporal lobe with executive processes. *NeuroImage*, *137*, 165–177. https://doi.org/10.1016/j.neuroimage.2016.05.051

Devlin, J. T., Russell, R. P., Davis, M. H., Price, C. J., Wilson, J., Moss, H. E., … Tyler, L. K. (2000). Susceptibility-Induced Loss of Signal: Comparing PET and fMRI on a Semantic Task. *NeuroImage*. https://doi.org/10.1006/nimg.2000.0595

Duncan, J. (2010). The multiple-demand (MD) system of the primate brain: mental programs for intelligent behaviour. Trends in Cognitive Sciences, 14(4), 172–179. https://doi.org/10.1016/j.tics.2010.01.004

Friedman, L., Glover, G. H., & The FBIRN Consortium. (2006). Reducing interscanner variability of activation in a multicenter fMRI study: Controlling for signal-to-fluctuation-noise-ratio (SFNR) differences. *NeuroImage*. https://doi.org/10.1016/j.neuroimage.2006.07.012

Friston, K. J., Fletcher, P., Josephs, O., Holmes, A., Rugg, M. D., & Turner, R. (1998). Event-related fMRI: characterizing differential responses. *NeuroImage*, *7*(1), 30–40. https://doi.org/10.1006/nimg.1997.0306

Geranmayeh, F., Brownsett, S. L. E., & Wise, R. J. S. (2014). Task-induced brain activity in aphasic stroke patients: what is driving recovery? Brain, 137, 2632–2648. https://doi.org/10.1093/brain/awu163

Gold, B. T., Balota, D. A., Jones, S. J., Powell, D. K., Smith, C. D., & Andersen, A. H. (2006). Dissociation of automatic and strategic lexical-semantics: functional magnetic resonance imaging evidence for differing roles of multiple frontotemporal regions. *The Journal of Neuroscience*, *26*(24), 6523–6532. https://doi.org/10.1523/JNEUROSCI.0808-06.2006

Goodglass H, Kaplan E. The assessment of aphasia and related disorders 2nd edn. Philadelphia, PA: Lea & Febiger; 1983

Gorgolewski, K. J., Lurie, D., Urchs, S., Kipping, J. A., Craddock, R. C., Milham, M. P., … Smallwood, J. (2014). A Correspondence between Individual Differences in the Brain's Intrinsic Functional Architecture and the Content and Form of Self-Generated Thoughts. *PLoS ONE*, *9*(5), e97176. https://doi.org/10.1371/journal.pone.0097176

Hall, D. A., Summerfield, A. Q., Gonçalves, M. S., Foster, J. R., Palmer, A. R., & Bowtell, R. W. (2000). Time-course of the auditory BOLD response to scanner noise. Magnetic Resonance in Medicine. https://doi.org/10.1002/(SICI)1522-2594(200004)43:4<601::AID-MRM16>3.0.CO;2-R

Hallam, G. P., Whitney, C., Hymers, M., Gouws, A. D., & Jefferies, E. (2016). Charting the effects of TMS with fMRI: Modulation of cortical recruitment within the distributed network supporting semantic control. *Neuropsychologia*, *93*, 40–52. https://doi.org/10.1016/j.neuropsychologia.2016.09.012

Hoffman, P., Jefferies, E., & Lambon Ralph, M. a. (2010). Ventrolateral prefrontal cortex plays an executive regulation role in comprehension of abstract words: convergent neuropsychological and repetitive TMS evidence. *The Journal of Neuroscience*, *30*(46), 15450–15456. https://doi.org/10.1523/JNEUROSCI.3783-10.2010

Hoffman, P., Rogers, T. T., & Lambon Ralph, M. A. (2011). Semantic Diversity Accounts for the "Missing" Word Frequency Effect in Stroke Aphasia: Insights Using a Novel Method to Quantify Contextual Variability in Meaning. *Journal of Cognitive Neuroscience*, *23*(9), 2432–2446. https://doi.org/10.1162/jocn.2011.21614

Hymers, M., Prendergast, G., Liu, C., Schulze, A., Young, M. L., Wastling, S. J., … Millman, R. E. (2015). Neural mechanisms underlying song and speech perception can be differentiated using an illusory percept. *NeuroImage*, *108*, 225–33. https://doi.org/10.1016/j.neuroimage.2014.12.010

Jackson, R. L., Hoffman, P., Pobric, G., & Lambon Ralph, M. A. (2016). The Semantic Network at Work and Rest: Differential Connectivity of Anterior Temporal Lobe Subregions. Journal of Neuroscience. https://doi.org/10.1523/JNEUROSCI.2999-15.2016

Jefferies, E., & Lambon Ralph, M. A. (2006). Semantic impairment in stroke aphasia versus semantic dementia: A case-series comparison. *Brain*, *129*(Pt 8), 2132–2147. Retrieved from http://dx.doi.org/10.1093/brain/awl153

Jefferies, E. (2013). The neural basis of semantic cognition: converging evidence from neuropsychology, neuroimaging and TMS. *Cortex*, *49*(3), 611–625. https://doi.org/10.1016/j.cortex.2012.10.008

Jefferies, E., Baker, S. S., Doran, M., & Ralph, M. A. L. (2007). Refractory effects in stroke aphasia: A consequence of poor semantic control. *Neuropsychologia*, *45*(5), 1065–1079. https://doi.org/10.1016/j.neuropsychologia.2006.09.009

Jenkinson, M., Bannister, P., Brady, M., & Smith, S. (2002). Improved Optimization for the Robust and Accurate Linear Registration and Motion Correction of Brain Images. *NeuroImage*, *17*(2), 825–841. https://doi.org/10.1006/nimg.2002.1132

Jenkinson, M., & Smith, S. (2001). A global optimisation method for robust affine registration of brain images. *Medical Image Analysis*, *5*(2), 143–156. https://doi.org/10.1016/S1361-8415(01)00036-6

Jung, J., & Lambon Ralph, M. A. (2016). Mapping the Dynamic Network Interactions Underpinning Cognition: A cTBS-fMRI Study of the Flexible Adaptive Neural System for Semantics. *Cerebral Cortex*, *26*(8), 3580–3590. https://doi.org/10.1093/cercor/bhw149

Kay J, Lesser R, Coltheart M. Psycholinguistic assessments of language processing in aphasia (PALPA). Hove: Lawrence Erlbaum Associates; 1992.

Lambon Ralph, M. A., Jefferies, E., Patterson, K., & Rogers, T. T. (2017). The neural and computational bases of semantic cognition. *Nature Reviews Neuroscience*, *18*(1), 42–55. https://doi.org/10.1038/nrn.2016.150

Mueller, K., Mildner, T., Fritz, T., Lepsien, J., Schwarzbauer, C., Schroeter, M. L., & Möller, H. E. (2011). Investigating brain response to music: a comparison of different fMRI acquisition schemes. *NeuroImage*, *54*(1), 337–43. https://doi.org/10.1016/j.neuroimage.2010.08.029

Murphy, K., Birn, R. M., Handwerker, D. A., Jones, T. B., & Bandettini, P. A. (2009). The impact of global signal regression on resting state correlations: Are anti-correlated networks introduced? *NeuroImage*, *44*(3), 893–905. https://doi.org/10.1016/j.neuroimage.2008.09.036

Murphy, C., Rueschemeyer, S. A., Watson, D., Karapanagiotidis, T., Smallwood, J., & Jefferies, E. (2017). Fractionating the anterior temporal lobe: MVPA reveals differential responses to input and conceptual modality. NeuroImage. https://doi.org/10.1016/j.neuroimage.2016.11.067

Nachev, P., Coulthard, E., Jäger, H. R., Kennard, C., & Husain, M. (2008). Enantiomorphic normalization of focally lesioned brains. *NeuroImage*, *39*(3), 1215–1226. https://doi.org/10.1016/j.neuroimage.2007.10.002

Noonan, K. A., Jefferies, E., Visser, M., & Lambon Ralph, M. a. (2013). Going beyond inferior prefrontal involvement in semantic control: evidence for the additional contribution of dorsal angular gyrus and posterior middle temporal cortex. *Journal of Cognitive Neuroscience*, *25*(11), 1824–1850. https://doi.org/10.1162/jocn_a_00442

Nooner, K. B., Colcombe, S. J., Tobe, R. H., Mennes, M., Benedict, M. M., Moreno, A. L., … Milham, M. P. (2012). The NKI-Rockland Sample: A Model for Accelerating the Pace of Discovery Science in Psychiatry. *Frontiers in Neuroscience*, *6*, 152. https://doi.org/10.3389/fnins.2012.00152

Patterson, K., Nestor, P. J., & Rogers, T. T. (2007). Where do you know what you know? The representation of semantic knowledge in the human brain. *Nature Reviews Neuroscience*, *8*(12), 976–987. https://doi.org/10.1038/nrn2277

Raven JC. Coloured progressive matrices sets A, AB, B. London: H. K. Lewis.; 1962.

Robson, H., Zahn, R., Keidel, J. L., Binney, R. J., Sage, K., & Lambon Ralph, M. A. (2014). The anterior temporal lobes support residual comprehension in Wernicke's aphasia. *Brain*, *137*(3), 931–943. https://doi.org/10.1093/brain/awt373

Rodd, J. M., Davis, M. H., & Johnsrude, I. S. (2005). The neural mechanisms of speech comprehension: fMRI studies of semantic ambiguity. *Cerebral Cortex*, *15*(8), 1261–1269. https://doi.org/10.1093/cercor/bhi009

Rodd, J. M., Johnsrude, I. S., & Davis, M. H. (2012). Dissociating frontotemporal contributions to semantic ambiguity resolution in spoken sentences. *Cerebral Cortex*, *22*(8), 1761–73. https://doi.org/10.1093/cercor/bhr252

Rodd, J. M., Vitello, S., Woollams, A. M., & Adank, P. (2015). Localising semantic and syntactic processing in spoken and written language comprehension: an Activation Likelihood Estimation meta-analysis. Brain and Language, 141, 89–102. https://doi.org/10.1016/j.bandl.2014.11.012

Rogers, T. T., Patterson, K., Jefferies, E., & Lambon Ralph, M. A. (2015). Disorders of representation and control in semantic cognition: Effects of familiarity, typicality, and specificity. *Neuropsychologia*, *76*, 220–239. https://doi.org/10.1016/j.neuropsychologia.2015.04.015

Rorden, C., Bonilha, L., Fridriksson, J., Bender, B., & Karnath, H. O. (2012). Age-specific CT and MRI templates for spatial normalization. *NeuroImage*, *61*(4), 957–965. https://doi.org/10.1016/j.neuroimage.2012.03.020

Schwarzbauer, C., Davis, M. H., Rodd, J. M., & Johnsrude, I. (2006). Interleaved silent steady state (ISSS) imaging: a new sparse imaging method applied to auditory fMRI. *NeuroImage*, *29*(3), 774–82. https://doi.org/10.1016/j.neuroimage.2005.08.025

Scott, S. K., Blank, C. C., Rosen, S., & Wise, R. J. S. (2000). Identification of a pathway for intelligible speech in the left temporal lobe. *Brain*, *123*(12), 2400–2406. https://doi.org/10.1093/brain/123.12.2400

Smallwood, J., Karapanagiotidis, T., Ruby, F., Medea, B., de Caso, I., Konishi, M., … Jefferies, E. (2016). Representing Representation: Integration between the Temporal Lobe and the Posterior Cingulate Influences the Content and Form of Spontaneous Thought. *PLOS ONE*, *11*(4), e0152272. https://doi.org/10.1371/journal.pone.0152272

Smith, S. M. (2002). Fast robust automated brain extraction. *Human Brain Mapping*, *17*(3), 143–55. https://doi.org/10.1002/hbm.10062

Thompson, H. E., Robson, H., Lambon Ralph, M. A., & Jefferies, E. (2015). Varieties of semantic "access" deficit in Wernicke's aphasia and semantic aphasia. *Brain*, *138*(12), 3776–3792. https://doi.org/10.1093/brain/awv281

Thompson-Schill, S. L., D'Esposito, M., Aguirre, G. K., & Farah, M. J. (1997). Role of left inferior prefrontal cortex in retrieval of semantic knowledge: A reevaluation. *Proceedings of the National Academy of Sciences*, *94*(26), 14792–14797. https://doi.org/10.1073/pnas.94.26.14792

Visser, M., Jefferies, E., & Lambon Ralph, M. A. (2010). Semantic Processing in the Anterior Temporal Lobes: A Meta-analysis of the Functional Neuroimaging Literature. Journal of Cognitive Neuroscience. https://doi.org/10.1162/jocn.2009.21309

Vitello, S., Warren, J. E., Devlin, J. T., & Rodd, J. M. (2014). Roles of frontal and temporal regions in reinterpreting semantically ambiguous sentences. *Frontiers in Human Neuroscience*, *8*(July), 530. https://doi.org/10.3389/fnhum.2014.00530

Warrington, E. K., & Cipolotti, L. (1996). Word comprehension: The distinction between refractory and storage impairments. *Brain*, *119*(2), 611–625. https://doi.org/10.1093/brain/119.2.611

Whitney, C., Jefferies, E., & Kircher, T. (2011). Heterogeneity of the left temporal lobe in semantic representation and control: Priming multiple versus single meanings of ambiguous words. *Cerebral Cortex*, *21*(4), 831–844. https://doi.org/10.1093/cercor/bhq148

Whitney, C., Kirk, M., O'Sullivan, J., Lambon Ralph, M. A., & Jefferies, E. (2011). The neural organization of semantic control: TMS evidence for a distributed network in left inferior frontal and posterior middle temporal gyrus.

Cerebral Cortex, *21*(5), 1066–1075. https://doi.org/10.1093/cercor/bhq180

Woolrich, M. W., Behrens, T. E. J., Beckmann, C. F., Jenkinson, M., & Smith, S. M. (2004). Multilevel linear modelling for FMRI group analysis using Bayesian inference. *NeuroImage*, *21*(4), 1732–47. https://doi.org/10.1016/j.neuroimage.2003.12.023

Yarkoni, T., Poldrack, R. A., Nichols, T. E., Van Essen, D. C., & Wager, T. D. (2011). Large-scale automated synthesis of human functional neuroimaging data. *Nature Methods*, *8*(8), 665–670. https://doi.org/10.1038/nmeth.1635

Figure S1: Stroke lesion overlap map for the group of 14 patients

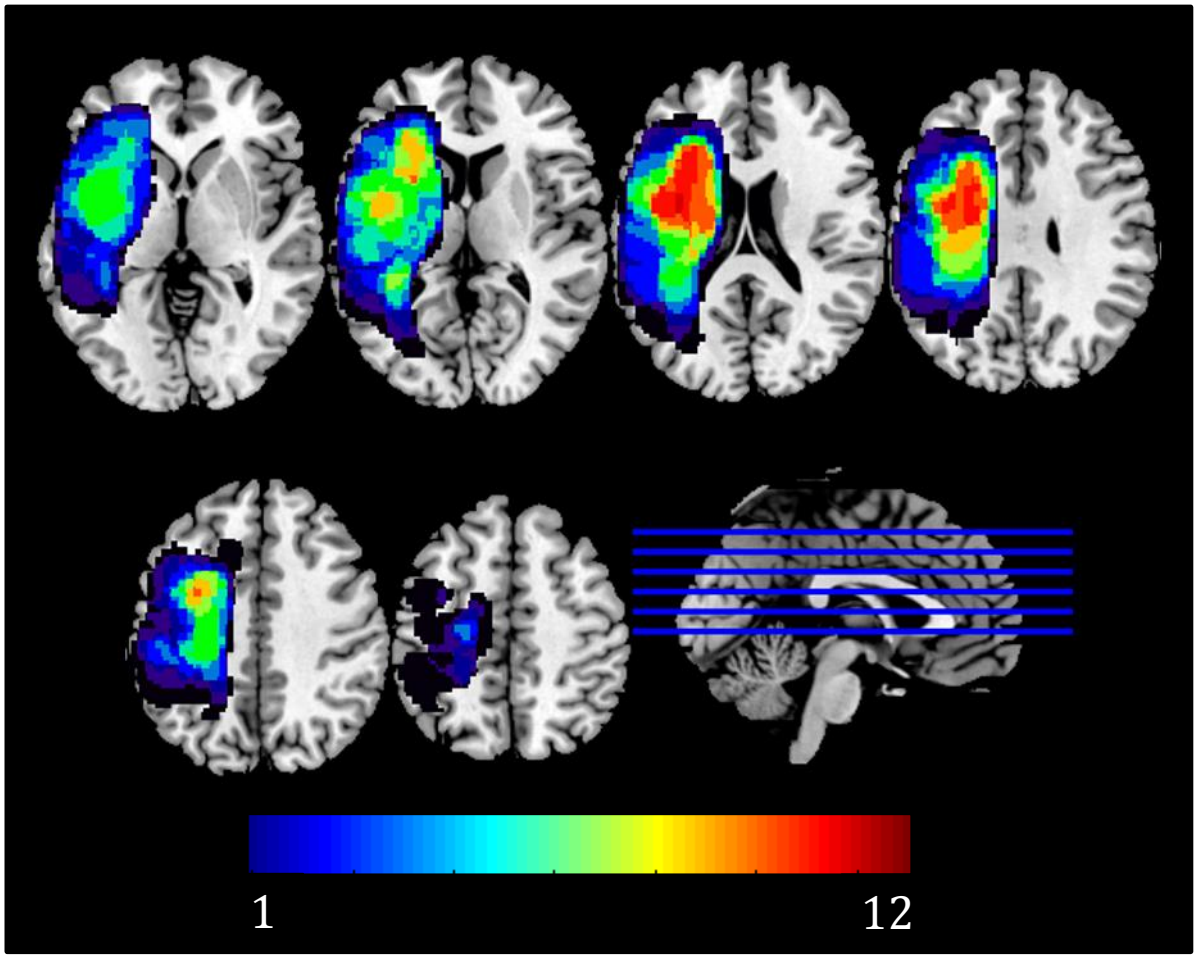

Table S1: Connectivity of the lesion mask

		Z	x	y	z	Voxels
Positive connectivity						
L	Central operculum	11.9	-44	6	10	13826
L	Anterior insula	7.92	-36	22	0	
L	Inferior frontal gyrus (pars triangularis)	7.86	-38	28	4	
L	Inferior frontal gyrus (pars triangularis)	7.82	-44	30	2	
L	Anterior insula	7.72	-28	22	6	
L	Inferior frontal gyrus (pars triangularis)	7.4	-42	22	6	
R	Mid insula	7.04	38	2	8	3827
R	Precentral gyrus	6.72	48	8	8	
R	Inferior frontal gyrus (pars triangularis)	5.13	48	32	2	
R	Anterior insula	4.99	36	24	-2	
R	Anterior insula	4.95	36	28	4	
R	Inferior frontal gyrus (pars triangularis)	4.74	42	30	2	
L	Pre supplementary motor area	6.46	-4	14	42	
L	Pre supplementary motor area	6.33	-6	18	50	
L	Pre supplementary motor area	6.15	-4	2	54	
L	Anterior cingulate	5.4	-8	16	34	
L	Anterior cingulate	4.22	-10	32	22	
L	Anterior cingulate	4.14	-8	32	18	
L	Thalamus	6.09	-10	-8	6	699
L	Thalamus	5.34	-4	-20	2	
L	Substantia nigra	3.61	-8	-20	-12	
L	Thalamus	3.08	-10	-30	-2	
L	Peri-acqueductal grey	2.75	-6	-26	-16	
R	Supramarginal gyrus	4.39	62	-32	46	661
R	Supramarginal gyrus	4.1	66	-42	26	
R	Supramarginal gyrus	4.07	64	-28	40	
R	Supramarginal gyrus	4.05	60	-38	48	
R	Supramarginal gyrus	3.67	58	-26	50	
R	Central operculum	3.23	62	-20	20	
L	Inferior temporal gyrus / anterior temporal lobe	4.18	-42	-6	-42	522
L	Inferior temporal gyrus / anterior temporal lobe	4.12	-34	-6	-44	
L	Temporal fusiform cortex	4.11	-32	-18	-34	
L	Temporal pole	3.44	-26	4	-42	
L	Temporal pole	3.1	-28	10	-40	
L	Temporal pole	2.82	-34	8	-44	
Negative connectivity						
R	Posterior cingulate	6.65	10	-44	30	11816

R	Posterior cingulate	6.54	8	-40	30	
L	Posterior cingulate	6.12	-18	-54	8	
R	Posterior cingulate	6.07	2	-46	32	
R	Precuneous	5.88	2	-66	58	
R	Posterior cingulate	5.78	6	-48	32	
R	Frontal pole	5.05	4	64	-10	2303
R	Frontal pole	4.74	4	56	-18	
R	Dorso-medial prefrontal cortex	4.72	4	52	-12	
R	Frontal pole	4.66	6	50	-28	
R	Dorso-medial prefrontal cortex	4.61	4	44	-12	
	Para-cingulate gyrus	4.48	0	38	-12	
R	Middle temporal gyrus	4.7	62	-14	-18	891
R	Inferior temporal gyrus	4.3	56	-20	-24	
R	Middle temporal gyrus	4.24	62	-14	-8	
R	Middle temporal gyrus	3.67	54	-10	-28	
R	Inferior temporal gyrus	3.47	62	-12	-32	
R	Middle temporal gyrus	3.32	60	-22	-16	
R	Middle frontal gyrus	4.95	24	30	38	732
R	Middle frontal gyrus	4.88	24	32	42	
R	Middle frontal gyrus	4.4	26	18	44	
R	Middle frontal gyrus	4.36	26	22	42	
R	Middle frontal gyrus	3.7	36	6	50	
R	Middle frontal gyrus	3.42	36	24	40	

Table S2: Sentences > noise for patients and controls (masked by Neurosynth 'semantic' map)

		Z	x	y	z	Voxels
Patients						
L	Inferior anterior temporal lobe	11.8	-36	-8	-38	5098
L	Inferior anterior temporal lobe	10.4	-36	-6	-34	
L	Posterior middle temporal gyrus	7.94	-58	-40	-12	
L	Parahippocampal gyrus	6.83	-30	-20	-32	
L	Anterior middle temporal gyrus	6.72	-60	-10	-26	
L	Posterior superior temporal gyrus	6.68	-52	-18	-6	
Controls						
L	Inferior anterior temporal lobe	9.32	-46	0	-36	6218
L	Temporal pole	7.27	-52	4	-40	
L	Temporal pole	6.65	-48	4	-18	
L	Planum polare	6.31	-48	4	-14	
L	Inferior frontal gyrus pars triangularis	6.15	-42	28	-4	
L	Temporal pole	5.88	-46	6	-36	

Table S3: Functional connectivity of left pMTG and vATL in patients and controls

		Z	x	y	z	Voxels
Patients LpMTG						
L	Posterior middle temporal gyrus	6.99	-58	-54	-10	
L	Posterior inferior temporal gyrus	5.35	-62	-46	-16	
L	Posterior middle temporal gyrus	5.33	-50	-62	0	
L	Posterior middle temporal gyrus	3.93	-54	-36	-6	
L	Lateral occipital cortex	3.7	-50	-68	-8	
L	Posterior temporal fusiform cortex	3.35	-42	-36	-18	
R	Posterior inferior temporal gyrus	4.57	56	-58	-10	
R	Posterior middle temporal gyrus	4.06	62	-54	-10	
R	Posterior inferior temporal gyrus	3.61	62	-46	-14	
R	Posterior inferior temporal gyrus	3.6	58	-44	-12	
R	Posterior inferior temporal gyrus	3.12	48	-48	-34	
R	Posterior middle temporal gyrus	3.08	70	-34	-8	
L	Superior lateral occipital cortex	2	-14	-72	46	
L	Superior lateral occipital cortex	3.84	-32	-86	26	
L	Superior lateral occipital cortex	3.38	-28	-76	38	
L	Superior lateral occipital cortex	2.92	-28	-72	30	
L	Superior lateral occipital cortex	2.9	-20	-66	52	
L	Superior lateral occipital cortex	2.37	-24	-64	46	
R	Cerebellum	3.55	38	-68	-38	
R	Cerebellum	3.39	28	-76	-48	
R	Cerebellum	3.27	20	-76	-52	
R	Cerebellum	2.4	36	-66	-56	
Patients LATL						
R	Anterior temporal fusiform cortex	4.44	36	-6	-44	2214
R	Posterior temporal fusiform cortex	4.29	28	-12	-40	
R	Parahippocampal gyrus	4.27	30	2	-28	
R	Frontal pole	3.98	26	30	-20	
R	Posterior temporal fusiform cortex	3.94	36	-16	-30	
R	Anterior parahippocampal gyrus	3.92	22	4	-26	
L	Anterior temporal fusiform cortex	6.49	-38	-10	-38	1818
L	Anterior parahippocampal gyrus	5.56	-30	-12	-36	
L	Anterior inferior temporal gyrus	4.83	-42	-8	-44	
L	Anterior inferior temporal gyrus	4.55	-48	-2	-40	
L	Temporal pole	4.38	-38	18	-36	
L	Anterior temporal fusiform cortex	3.93	-32	-8	-48	
Controls LpMTG						
L	Posterior middle temporal gyrus	6.47	-56	-56	-8	3013
L	Posterior middle temporal gyrus	5.28	-56	-56	2	
L	Posterior middle temporal gyrus	4.68	-62	-44	-14	
L	Inferior lateral occipital cortex	4.64	-50	-70	-4	
L	Posterior middle temporal gyrus	4.41	-66	-46	0	
L	Posterior superior temporal gyrus	4.27	-60	-40	14	
R	Posterior inferior temporal gyrus	4.27	60	-42	-22	1170

R	Posterior middle temporal gyrus	4.14	54	-48	-4	
R	Posterior middle temporal gyrus	4	64	-54	-8	
R	Posterior inferior temporal gyrus	3.56	48	-56	-12	
R	Posterior inferior temporal gyrus	3.41	66	-40	-16	
R	Inferior lateral occipital cortex	2.89	46	-74	-8	
R	Frontal pole	5.06	-46	36	-6	852
R	Middle frontal gyrus	3.34	-40	12	38	
R	Middle frontal gyrus	3.03	-50	20	28	
R	Orbitofrontal cortex	3.01	-48	24	-6	
R	Inferior frontal gyrus (pars opercularis)	2.98	-50	14	2	
R	Inferior frontal gyrus (pars triangularis)	2.81	-52	28	24	
Controls LATL						
L	Anterior inferior temporal gyrus	6.74	-42	-8	-36	2620
L	Posterior temporal fusiform cortex	6.72	-36	-12	-32	
L	Posterior temporal fusiform cortex	6.58	-38	-10	-36	
L	Temporal pole	4.61	-40	12	-28	
L	Temporal pole	4.33	-38	12	-24	
L	Anterior parahippocampal gyrus	4.25	-22	-12	-30	
R	Anterior temporal fusiform cortex	4.83	38	-4	-38	2211
R	Temporal pole	4.6	52	10	-18	
R	Anterior parahippocampal gyrus	4.49	22	4	-28	
R	Hippocampus	4.47	18	-18	-20	
R	Amygdala	4.44	20	0	-26	
R	Posterior superior temporal gyrus	4.41	50	-12	-8	
R	Periaqueductal grey	4.99	2	-28	-36	420
R	Brain stem	3.92	6	-40	-32	
R	Brain stem	3.65	6	-28	-44	
R	Brain stem	3.65	6	-38	-52	
L	Brain stem	3.52	-4	-30	-42	
R	Cerebellum	3.48	26	-42	-34	

Table S4: Task x group interaction using pMTG ROI as an explanatory variable in a group-level regression of resting-state functional connectivity

Ambiguity x group LpMTG interaction						
L	Temporal pole	4.44	-40	24	-18	
L	Temporal pole	4.17	-46	16	-22	
L	Temporal pole	4.13	-42	18	-22	
L	Temporal pole	4.12	-42	8	-28	
L	Temporal pole	3.81	-46	12	-28	
L	Orbitofrontal cortex	3.26	-26	14	-22	